arXiv:cond-mat/0303286v3 [cond-mat.stat-mech] 26 Oct 2003

Specific heats of dilute neon inside long single-walled carbon nanotube

Z. C. Tu†‡* and Z. C. Ou-Yang†§

† Institute of Theoretical Physics, The Chinese Academy of Sciences, P.O.Box 2735 Beijing 100080, China

‡ Graduate School, The Chinese Academy of Sciences, Beijing, China

§ Center for Advanced Study, Tsinghua University, Beijing 100084, China

Abstract. An elegant formula for coordinates of carbon atoms in a unit cell of a single-walled nanotube (SWNT) is presented and the potential of neon (Ne) inside an infinitely long SWNT is analytically derived out under the condition of the Lennard-Jones potential between Ne and carbon atoms. Specific heats of dilute Ne inside long (20, 20) SWNT are calculated at different temperatures. It is found that Ne exhibits 3-dimensional (3D) gas behavior at high temperature but behaves as 2D gas at low temperature. Especially, at ultra low temperature, Ne inside (20, 20) nanotubes behaves as lattice gas. A coarse method to determine the characteristic temperature $\mathcal{T}_c$ for low density gas in a potential is put forward. If $\mathcal{T} \gg \mathcal{T}_c$, we just need to use the classical statistical mechanics without solving the Shrödinger equation to consider the thermal behavior of gas in the potential. But if $\mathcal{T} \sim \mathcal{T}_c$, we must solve the Shrödinger equation. For Ne in (20,20) nanotube, we obtain $\mathcal{T}_c \approx 60$ K.

Submitted to: *J. Phys.: Condens. Matter*

PACS numbers: 61.46.+w, 82.60.Fa

* To whom correspondence should be addressed (tzc@itp.ac.cn)

1. Introduction

Since the discovery of carbon nanotubes [1], the peculiar electronic and mechanical properties of these structures have attracted much attention [2, 3, 4]. Experiments have also revealed that they can also be used to store hydrogen [5] and other gases [6]. Many physicists expected that gases in nanotubes or nanotube bundles may display novel 1-dimensional (1D) behavior as a consequence of the remarkable aspect ratio of the length of tubes to their radius. The group led by Cole [7] and other researchers [8] have theoretically studied properties of gases in nanotubes or nanotube bundles. One of the most fantastic properties they found is specific heat of dilute gas inside single-walled carbon nanotubes (SWNT's) as a functions of temperature: With temperature increasing it shows the thermal behavior changing from 1D, 2D, and 3D. However, there are still two question arisen: Do 1D and 2D behaviors always exist for dilute gas inside SWNT only if the temperature is low enough? Is classical statistical mechanics (CSM) sufficient to deal with this problem?

In Ref. [9], we has given a brief answer to the first question. Here we will exhibit the full calculations and continue to discuss the second question. In recent papers, Šiber *et al* treat the specific heat of dilute He atoms adsorbed in interstitial channels and grooves of carbon nanotube bundles [10]. Here we partially follow their aprroach.

This paper is organized as follows: In Sec.2, we give the expressions of the coordinates of carbon atoms in a unit cell of a SWNT. In Sec.7, we analytically calculate the potential of Ne in a carbon nanotube. For example, we calculate the potential of Ne in (20,20) tube. In Sec.4, we list the related formula of thermodynamics in statistical mechanics to calculate the specific heat. In Sec.5, we calculate the specific heats of Ne inside (20,20) at different temperatures without considering θ, z effects (θ, z are defined in Sec.2). In Sec.6, we calculate the specific heats of Ne inside (20,20) at low temperature. In Sec.7, we discuss why we do not use CSM to calculate the specific heat. In this section, we present a coarse method to estimate the characteristic temperature, below which the CSM can not be used. In Sec.8, we discuss the reliability of our results and give brief conclusions.

2. the coordinates of carbon atoms in a unit cell of a SWNT

A SWNT without two caps can be constructed by wrapping up a single sheet of graphite such that two equivalent sites of hexagonal lattice coincide [11]. To describe the SWNT, some characteristic vectors require introducing. As shown in Fig.1, the chiral vector $\mathbf{C}_h$, which defines the relative location of two sites, is specified by a pair of integers (n_1, n_2) which is called the index of the SWNT and relates $\mathbf{C}_h$ to two unit vectors $\mathbf{a}_1$ and $\mathbf{a}_2$ of graphite ($\mathbf{C}_h = n_1\mathbf{a}_1 + n_2\mathbf{a}_2$). The chiral angle θ_0 defines the angle between $\mathbf{a}_1$ and $\mathbf{C}_h$. For (n_1, n_2) nanotube, $\theta_0 = \arccos[\frac{2n_1+n_2}{2\sqrt{n_1^2+n_2^2+n_1n_2}}]$. The translational vector $\mathbf{T}$ corresponds to the first lattice point of 2D graphitic sheet through which the line normal to the chiral vector $\mathbf{C}_h$ passes. The unit cell of the SWNT is the rectangle

defined by vectors $\mathbf{C}_h$ and $\mathbf{T}$, while vectors $\mathbf{a}_1$ and $\mathbf{a}_2$ define the area of the unit cell of 2D graphite. The number N of hexagons per unit cell of SWNT is obtained as a function of n_1 and n_2 as $N = 2(n_1^2 + n_2^2 + n_1 n_2)/d_R$, where d_R is the greatest common divisor of $(2n_2 + n_1)$ and $(2n_1 + n_2)$. There are $2N$ carbon atoms in each unit cell of SWNT because every hexagon contains two atoms. To denote the $2N$ atoms, we use a symmetry vector $\mathbf{R}$ to generate coordinates of carbon atoms in the nanotube and is defined as the site vector having the smallest component in the direction of $\mathbf{C}_h$. From a geometric standpoint, vector $\mathbf{R}$ consists of a rotation around the nanotube axis by an angle $\Psi = 2\pi/N$ combined with a translation τ in the direction of $\mathbf{T}$; therefore, $\mathbf{R}$ can be denoted by $\mathbf{R} = (\Psi|\tau)$. Using the symmetry vector $\mathbf{R}$, we can divide the $2N$ carbon atoms in the unit cell of SWNT into two classes: one includes N atoms whose site vectors satisfy

$$\mathbf{A}_l = l\mathbf{R} - [l\mathbf{R} \cdot \mathbf{T}/\mathbf{T}^2]\mathbf{T} \quad (l = 0, 1, 2, \cdots, N-1), \tag{1}$$

another includes the remainder N atoms whose site vectors satisfy

$$\begin{aligned}\mathbf{B}_l &= l\mathbf{R} + \mathbf{B}_0 - [(l\mathbf{R} + \mathbf{B}_0) \cdot \mathbf{T}/\mathbf{T}^2]\mathbf{T} \\ &- [(l\mathbf{R} + \mathbf{B}_0) \cdot \mathbf{C}_h/\mathbf{C}_h^2]\mathbf{C}_h \quad (l = 0, 1, \cdots, N-1),\end{aligned} \tag{2}$$

where $\mathbf{B}_0 \equiv (\Psi_0|\tau_0) = \left(\frac{2\pi a_{cc}\cos(\theta_0 - \frac{\pi}{6})}{|\mathbf{C}_h|}\middle| a_{cc}\cos(\theta_0 - \frac{\pi}{6})\right)$ represents one of the nearest neighbor atoms to $\mathbf{A}_0$.

If we introduce a cylindrical coordinate system (r, θ, z) whose z-axis is the tube axis. Its $r\theta$-plane is perpendicular to z-axis and contains atom A_0 in the nanotube. r the distance from some point to z-axis, and θ the angle rotating around z-axis from an axis which is vertical to z-axis and passes through atom A_0 in the tube to the point. In this coordinate system, we can express Eqs.(1) and (2) as

$$\mathbf{A}_l = (\rho, l\Psi, l\tau - [l\tau/T]T) \quad (l = 0, 1, 2, \cdots, N-1), \tag{3}$$

and

$$\begin{aligned}\mathbf{B}_l = (&\rho, l\Psi + \Psi_0 - 2\pi[\frac{l\Psi + \Psi_0}{2\pi}], l\tau + \tau_0 - [\frac{l\tau + \tau_0}{T}]T) \\ &(l = 0, 1, 2, \cdots, N-1),\end{aligned} \tag{4}$$

where $\rho = \frac{|\mathbf{C}_h|}{2\pi}$. In Eqs.(1)-(4), the symbol $[\cdots]$ denotes the largest integer smaller than $\cdots$, e.g., $[5.3] = 5$.

3. the potential of ne inside carbon nanotubes

To obtain the potential of Ne inside the nanotube, we firstly consider another simple system shown in Fig. 2: Many atoms distribute regularly in a line form an infinite atom chain and an atom Q is out of the chain. The interval between neighbor atoms in the chain is T, and the site of atom Q relative to atom 0 can be represented by numbers c_1 and c_2. We take the Lennard-Jones potential $U(R_j) = 4\epsilon[(\sigma/R_j)^{12} - (\sigma/R_j)^6]$ between atom Q and atom j in the chain, where R_j is the distance between Q and atom j, and

$\epsilon = \sqrt{\epsilon_c \epsilon_{ne}}$, $\sigma = (\sigma_c + \sigma_{ne})/2$ with $\epsilon_{ne} = 35.6$ K, $\sigma_{ne} = 2.75$ Å, $\epsilon_c = 28$ K and $\sigma_c = 3.4$ Å[7, 12]. We calculate the potential between atom Q and the chain as

$$U_{QC} = 4\epsilon[\sigma^{12} U_6(c_1, c_2) - \sigma^6 U_3(c_1, c_2)], \tag{5}$$

where $U_k(c_1, c_2) = \sum_{n=-\infty}^{\infty} \frac{1}{[(c_1+nT)^2+c_2^2]^k}$ $(k = 1, 2, \cdots)$ which can be calculated through the following recursion [13]:

$$\begin{array}{l} U_1(c_1, c_2) = \frac{\pi \sinh(2\pi c_2/T)}{c_2 T[\cosh(2\pi c_2/T) - \cos(2\pi c_1/T)]}, \\ U_{k+1}(c_1, c_2) = -1/(2kc_2)\partial U_k/\partial c_2. \end{array} \tag{6}$$

The $(20, 20)$ tube, for example, with infinite length can be regarded as $2N = 80$ chains. Thus the potential of any point Q inside the tube can be calculated as

$$U(r, \theta, z) = \sum_{i=1}^{2N} U_{QC}, \tag{7}$$

where (r, θ, z) is coordinates of Q in the cylindrical coordinate system. As an approximation, we neglect the potential varying with z and θ because we find that it is much smaller than the potential varying with r through calculations, and fit the potential with $U(r) = 4\varepsilon[(\frac{\tilde{\sigma}}{\rho - r})^{10} - (\frac{\tilde{\sigma}}{\rho - r})^4]$, where $\rho = 13.56$ Å is the radius of the tube, $\varepsilon = 390$ K, and $\tilde{\sigma} = 2.63$ Å (see also Fig.3). Moreover, we simplify it as

$$U(r) = \begin{cases} 4\varepsilon[(\frac{\tilde{\sigma}}{\rho - r})^{10} - (\frac{\tilde{\sigma}}{\rho - r})^4], & r < \rho - \tilde{\sigma}, \\ \infty, & r > \rho - \tilde{\sigma}. \end{cases} \tag{8}$$

4. The basic formulae of thermodynamics in statistical mechanics

When we deal with the thermal behavior of dilute Ne in nanotube, we will begin with the free energy $\mathcal{F} = -\mathcal{T} \ln \mathcal{Z}$, where $\mathcal{T}$ is temperature and $\mathcal{Z} = \sum_n e^{-E_n/\mathcal{T}} = \mathrm{tr} \exp(-\mathcal{H}/\mathcal{T})$ is the partition function. We have let the Boltzmann factor be 1 [14]. E_n is the eigenvalues of the Schrödinger equation: $\mathcal{H}\psi_n = E_n \psi_n$. From the free energy, we can derive out the specific heat $c_v = -\mathcal{T}(\partial^2 \mathcal{F}/\partial \mathcal{T}^2)_v = \frac{\langle E_n^2 \rangle - \langle E_n \rangle^2}{\mathcal{T}^2}$, where $\langle E_n^2 \rangle = \sum_n E_n^2 e^{-E_n/\mathcal{T}}/\mathcal{Z}$ and $\langle E_n \rangle = \sum_n E_n e^{-E_n/\mathcal{T}}/\mathcal{Z}$.

We call above statistical mechanics ordinary statistics (OS) and list the corresponding formula in CSM: The free energy $\mathcal{F}_{cl} = -\mathcal{T} \ln \mathcal{Z}_{cl}$, where $\mathcal{Z}_{cl} = \int' e^{-E(p,q)/\mathcal{T}} d\Gamma$ is the partition function and here the prime means we integrate only over the regions of phase space which correspond to physically different states of particles. The specific heat $c_{vcl} = -\mathcal{T}(\partial^2 \mathcal{F}_{cl}/\partial \mathcal{T}^2)_v = \frac{\langle E^2 \rangle - \langle E \rangle^2}{\mathcal{T}^2}$, where $\langle E^2 \rangle = \int' E^2 e^{-E(p,q)/\mathcal{T}} d\Gamma/\mathcal{Z}_{cl}$ and $\langle E \rangle = \int' E e^{-E(p,q)/\mathcal{T}} d\Gamma/\mathcal{Z}_{cl}$.

Under the sufficient high temperature, $\mathcal{F}$ converge to the $\mathcal{F}_{cl}$. In other words, the applicable domain of $\mathcal{F}$ is larger than that of $\mathcal{F}_{cl}$. Therefore, the conclusion derived from $\mathcal{F}$ is much more reliable than that derived from $\mathcal{F}_{cl}$. We will use OS in the following discussions if we do not make special statement.

5. Specific Heats of Ne gas in an approximate potential

Because we consider the dilute Ne, we can neglect the interaction between Ne atoms and write the single particle Schrödinger equation [15] as $H\psi = E\psi$, where $H = -\frac{\hbar^2}{2\mu}\nabla^2 + U(r)$ and $\psi = \phi e^{i(m\theta+\kappa z)}$. It follows that

$$\begin{aligned} &E = \tfrac{\hbar^2\kappa^2}{2\mu} + E_m \quad (\kappa \in \mathbb{R}, m = 0, \pm1, \pm2, \cdots), \\ &H(r)\phi = E_m\phi, \\ &H(r) = -\tfrac{\hbar^2}{2\mu}(\tfrac{d^2}{dr^2} + \tfrac{1}{r}\tfrac{d}{dr} - \tfrac{m^2}{r^2}) + U(r), \end{aligned} \tag{9}$$

where m is angular quantum number and E_m is the corresponding energy. Setting $r = (\rho - \tilde{\sigma})\xi$, $\varepsilon_0 = \frac{\hbar^2}{2\mu\rho^2}$ and $\eta = \tilde{\sigma}/\rho$, Eqs.(8) and (9) are transformed into

$$u(\xi) = \begin{cases} 4\varepsilon[(\frac{\eta}{1-(1-\eta)\xi})^{10} - (\frac{\eta}{1-(1-\eta)\xi})^4], & \xi < 1, \\ \infty, & \xi > 1. \end{cases} \tag{10}$$

and

$$\begin{aligned} &\mathcal{H}\varphi(\xi) = E_m\varphi(\xi), \\ &\mathcal{H} = -\tfrac{\varepsilon_0}{(1-\eta)^2}(\tfrac{d^2}{d\xi^2} + \tfrac{1}{\xi}\tfrac{d}{d\xi} - \tfrac{m^2}{\xi^2}) + u(\xi). \end{aligned} \tag{11}$$

If we let $|\varphi\rangle = \sum_n a_n|\chi_n\rangle$, we will obtain the secular equation

$$det(\mathcal{H}_{jn} - E_m\mathcal{S}_{jn}) = 0, \tag{12}$$

where $\mathcal{H}_{jn} = \int_0^1 \chi_j\mathcal{H}(\xi)\chi_n\xi d\xi$, and $\mathcal{S}_{jn} = \int_0^1 \chi_j\chi_n\xi d\xi$. If we let $\chi_n = J_{|m|}(\nu_n\xi)$, where $J_{|m|}(\xi)$ is the m-th order Bessel function of the first class and ν_n is the n-th zero point of Bessel function [16], we can calculated $E_{mn}, (m = 0, \pm1, \pm2, \cdots; n = 1, 2, 3, \ldots)$ from Eq.(12).

If there are $\mathcal{N}$ Ne atoms inside the tube, we have the free energy $\mathcal{F} = -\mathcal{N}\mathcal{T}\ln\mathcal{Z}_1$, where $\mathcal{Z}_1 = \sum_{mn} e^{-E_{mn}/\mathcal{T}} \int_{-\infty}^{\infty} e^{-\frac{\hbar^2\kappa^2}{2\mu\mathcal{T}}} d\kappa$. We can easily obtain the specific heat per atom is

$$c_v = -\frac{\mathcal{T}\partial^2\mathcal{F}}{\mathcal{N}\partial\mathcal{T}^2} = \frac{1}{2} + \frac{\langle E_{nm}^2\rangle - \langle E_{nm}\rangle^2}{\mathcal{T}^2}, \tag{13}$$

where $\langle E_{nm}\rangle = \frac{\sum_{mn} E_{mn}e^{-Emn/\mathcal{T}}}{\sum_{mn} e^{-Emn/\mathcal{T}}}$ and $\langle E_{nm}^2\rangle = \frac{\sum_{mn} E_{mn}^2 e^{-Emn/\mathcal{T}}}{\sum_{mn} e^{-Emn/\mathcal{T}}}$.

In Fig.4, the symbols "∇" reflect c_v varying with the temperature $\mathcal{T}$, which implies Ne atoms inside (20,20) tube behave as 3D gas at high temperature (specific heat approaches to 3/2) and 2D gas at low temperature (specific heat is 1). Therefore, we can naturally assume that all atoms in the valley of potential $U(r)$ at low temperature, i.e. lie on the shell S^* with radius $\varrho = \rho[1 - (5/2)^{1/6}\eta]$.

At high temperature, the Ne atoms maybe evaporate from the nanotube, but our model cannot recover this effect because our potential is infinite near the surface of carbon nanotute.

6. Specific Heats at low temperature

Now we consider the thermal property of Ne inside the nanotube at low temperature in detail. We assume that all atoms lie on the shell S^* with radius $\varrho = \rho[1 - (5/2)^{1/6}\eta]$ at temperature lower than some critical temperature T_{lc} which depends on the energy difference between the tow lowest energy of radial excitations. From Eqs.(5)-(7) we can easily calculate the potential $U_s(v, z)$ on S^*, where $v = \varrho\theta$. The Hamiltonian of single particle can be expressed as $H' = -\frac{\hbar^2}{2\mu}(\frac{\partial^2}{\partial v^2} + \frac{\partial^2}{\partial z^2}) + U_s(v, z)$.

In fact, U_s has periodic structure. If we denote $\boldsymbol{\alpha}_1 = (2\pi\varrho/N, \tau)$, $\boldsymbol{\alpha}_2 = (0, T)$ and $\boldsymbol{\gamma}_l = l_1\boldsymbol{\alpha}_1 + l_2\boldsymbol{\alpha}_2$, we have $U_s(\mathbf{r} + \boldsymbol{\gamma}_l) = U_s(\mathbf{r})$, where $l_1, l_2 \in \mathbb{Z}$ and $\mathbf{r} = (v, z)$. On the one hand, we have the Bloch's theorem [17]:

$$\begin{aligned} &H'\Phi(\boldsymbol{\kappa}, \mathbf{r}) = E_{\boldsymbol{\kappa}}\Phi(\boldsymbol{\kappa}, \mathbf{r}), \\ &\Phi(\boldsymbol{\kappa}, \mathbf{r} + \boldsymbol{\gamma}_l) = e^{i\boldsymbol{\kappa}\cdot\boldsymbol{\gamma}_l}\Phi(\boldsymbol{\kappa}, \mathbf{r}), \end{aligned} \tag{14}$$

which suggests that $\Phi(\boldsymbol{\kappa}, \mathbf{r}) = \sum_j a(\boldsymbol{\kappa} + \mathbf{G}_j)e^{i(\boldsymbol{\kappa}+\mathbf{G}_j)\cdot\mathbf{r}}$, where $\mathbf{G}_j = j_1\boldsymbol{\beta}_1 + j_2\boldsymbol{\beta}_2$ with $j_1, j_2 \in \mathbb{Z}$, $\boldsymbol{\beta}_1 = (N/\varrho, 0)$ and $\boldsymbol{\beta}_2 = (-\tau N/(T\varrho), 2\pi/T)$. From Eq.(30), we obtain the secular equation

$$det(\mathcal{H}_{lj} - E_{\boldsymbol{\kappa}}\delta_{lj}) = 0, \tag{15}$$

where $\mathcal{H}_{lj} = \frac{\hbar^2}{2\mu}(\boldsymbol{\kappa} + \mathbf{G}_j)^2\delta_{lj} + \mathcal{U}_{lj}$, $\mathcal{U}_{lj} = \frac{1}{\Omega_0}\int_{\Omega_0} e^{i(\mathbf{G}_l - \mathbf{G}_j)\cdot\mathbf{r}}U_s(\mathbf{r})d\mathbf{r}$ and $\Omega_0 = |\boldsymbol{\alpha}_1 \times \boldsymbol{\alpha}_2|$.

On the other hand, Periodic boundary condition along the circumference of the shell S^* suggests that we just need to consider the first Brillouin zone which consists of $\boldsymbol{\kappa} = (m_v/\varrho, \kappa_z)$ where $m_v \in \mathbb{Z}, 0 \le m_v < N$ and $\kappa_z \in \mathbb{R}, 0 \le \kappa_z < 2\pi/T$.

From Eq.(15), we can calculate the energy E_{m_v,κ_z}, and then the free energy $\mathcal{F} = -\mathcal{N}\mathcal{T}\ln\mathcal{Z}_1$ [18], where $\mathcal{Z}_1 = \sum_{m_v}\int_0^{2\pi/T} e^{-E_{m_v,\kappa_z}/\mathcal{T}}d\kappa_z$. Moreover, the specific heat per atom is [14]

$$c_v = -\frac{\mathcal{T}\partial^2\mathcal{F}}{\mathcal{N}\partial\mathcal{T}^2} = \frac{\langle E'^2\rangle - \langle E'\rangle^2}{\mathcal{T}^2}, \tag{16}$$

where $\langle E'\rangle = \sum_{m_v=0}^{N-1}\int_0^{2\pi/T} E_{m_v,\kappa_z}e^{-E_{m_v,\kappa_z}/\mathcal{T}}d\kappa_z/\mathcal{Z}$ and $\langle E'^2\rangle = \sum_{m_v=0}^{N-1}\int_0^{2\pi/T} E^2_{m_v,\kappa_z}e^{-E_{m_v,\kappa_z}/\mathcal{T}}d\kappa_z/\mathcal{Z}$.

In Fig.5, the symbols "∇" reflect c_v varying with the temperature $\mathcal{T}$, which implies Ne atoms inside (20,20) tube behave as the lattice gas [19] at ultra low temperature (specific heat is 0) and 2D gas at low temperature (specific heat approaches 1). There is no 1D gas inside (20,20) tube, which is quite different from our usual notion.

7. why not use CSM?

At the sufficient high temperature, $\mathcal{F}$ converge to the $\mathcal{F}_{cl}$. If a carbon nanotube, for example (20, 20) tube, just a geometric tube with diameter $d \approx 2$ nm, the characteristic temperature $\mathcal{T}_c = h^2/(2\pi md^2) = 0.04$ K. We just need to use the CSM if $\mathcal{T} >> \mathcal{T}_c$. However, here the carbon nanotube provides potential to Ne. In the potential, it is difficult matter to calculate the characteristic temperature is not a simple matter. For example, consider some atoms in a harmonic potential $U(r) = \frac{1}{2}m\omega^2r^2$. We can easily

calculate the specific heat per atom $c_v = (3\omega^2/\mathcal{T}^2)\exp(-\omega/\mathcal{T})/[1-\exp(-\omega/\mathcal{T})]^2$ [14]. Here we have set $\hbar = 1$. We know $c_v = 3$ if $\mathcal{T} >> \omega$ and this is the classical case. Thus we can set $\mathcal{T}_c = \omega$ (In the whole form $\mathcal{T}_c = \hbar\omega/k_B$). Above discussion suggests that $\mathcal{T}_c$ depends on the potential. We propose a coarse method to obtain $\mathcal{T}_c$ which is the least root of the following equation:

$$\begin{cases} U_m + \mathcal{T}_c = U(R_1) = U(R_2) \\ R_2 - R_1 = h/\sqrt{2\pi m \mathcal{T}_c} \end{cases} . \tag{17}$$

The physical meanings of parameters in Eq.(17) are shown in the Fig.6.

For the potential $U(r) = \frac{1}{2}m\omega^2 r^2$ in above example, $U_m = 0, R_1 = -R_2, R_2 - R_1 = 2R_2$, using Eq.(17) we arrive at $\mathcal{T}_c = \frac{\sqrt{\pi}}{2}\omega \sim \omega$ (the whole form is $\mathcal{T}_c = \frac{\sqrt{\pi}\hbar\omega}{2k_B} \sim \hbar\omega/k_B$). For (20,20) nanotube, the approximate potential is $U(r) = 4\varepsilon[(\frac{\tilde{\sigma}}{\rho-r})^{10} - (\frac{\tilde{\sigma}}{\rho-r})^4]$, with $\rho = 13.56$ Å, $\varepsilon = 390$ K, and $\tilde{\sigma} = 2.63$ Å. We can numerical solve Eq.(17) and give $\mathcal{T}_c \approx 60$ K. If $\mathcal{T} >> \mathcal{T}_c$ (e.g. $\mathcal{T} > 3\mathcal{T}_c = 180$ K), the classical case is expected and CSM is valid. But CSM can not be used if $\mathcal{T} \sim \mathcal{T}_c$ (e.g. $\mathcal{T} < 2\mathcal{T}_c = 120$ K), especially $\mathcal{T} < \mathcal{T}_c = 60$ K.

In Fig.4 we give results obtained from OS and CSM. The information shown in Fig.4 agrees with our coarse estimate to $\mathcal{T}_c$ very well. Therefore, using the CMS is insufficient. It is necessary to consider the quantum mechanics. In other words, quantum mechanics must be used when studying the behaviors of gases in the nanometer scale.

8. discussion and conclusion

We notice that the potential U is a function of (r, θ, z) and $U(r, \theta + 2\pi j_1/N, z + j_1\tau + j_2 T) = U(r, \theta, z)$, where N, τ, T are parameters of a carbon nanotube, and j_1, j_2 are two integers. Under this symmetry, we must use a generalized Bloch's theorem (see appendix) to find the eigenvalues of Schrödinger equation. We can also obtain the secular equation of energies. Although we have 16 Pentium IV computers, but the data and computing time exceed our computers' ability if we calculate the specific heat with temperature varying from 0 to 400 K. But, fortunately, we find that the variation of potential with θ, z is less than 30 K, much smaller than that with r. In Sec.5, we neglect the effect of the variation of potential with θ, z. Indeed, this effect can be neglected under high temperature in terms of intuition. At high temperature, the values of c_v approach to that calculated from CSM. We show them in Fig.7, in which the triangles are values neglected the effect of θ, z and the line is the result calculated from CSM considering the effect of θ, z. It suggests our intuition is reliable.

We know the effect of θ, z is important under the low temperature. In Sec.6, we consider this effect in detail. Because the shape of U is very sharp and deep with r, the particles are confined in the bottom of $U(r)$ at low temperature. Thus we can consider the effect of θ, z but neglect the effect of r at low temperature.

Therefore, we believe that we have grasped the main factors under at high and low temperature and our qualitative conclusions are reliable.

The interactions (include the contribution from the polarization of the pi-electrons) between Ne and C atoms are intermolecular forces, van der Waals type interactions. As the theoretical study, the simplest form of van der Waals force is the Lenard-Jones potential. We believe that the eventual results based on the Lenard-Jones potential are qualitatively reasonable. Maybe, many researchers [7, 8] use it because of the same reasons. Indeed, the more detailed study needs to consider the Gay-Berne potential [20] or other complex potentials. We are considering to overcome this difficult problem by using numerical simulations.

It is necessary to notice that we just consider the dilute Ne and the interactions between Ne atoms are naturally neglected. Therefore we do not describe the phase transition of Ne in SWNT's. If we intend to deal with the phase transition, we must include the interactions between Ne atoms and use the methods of quantum field theory, such as the renormalization group approach [21], etc.

In conclusion, we calculate the specific heat of Ne in (20,20) SWNT at low and high temperature and find the dimensional crossover of thermal behavior in this system. Especially, the dilute Ne gas exhibits as 2D behavior at low temperature or 2D lattice behavior at ultra low temperature. The simple physical picture is that all atoms are confined on a shell blow a critical temperature.

Acknowledgments

We are grateful to kind discussion of Prof. H. W. Peng, Dr. R. An, M. Li, Y. Zhang, and L. R. Dai.

Appendix: Generalized Bloch's theorem

In Sec.5, we calculate the specific heat with neglecting the effect of θ, z; and in Sec.6, in fact, we neglect the effect of r. In other words, we do not obtain the specific heats in a consistent way from low to high temperature. Indeed, the potential U is a function of (r, θ, z) and satisfies $U(r, \theta + 2\pi j_1/N, z + j_1\tau + j_2 T) = U(r, \theta, z)$, where j_1, j_2 are two integers. If a potential satisfies this condition, it is called the spiral symmetric. Under this spiral symmetry, we must use a generalized Bloch's theorem to find the eigenvalues of Schrödinger equation and then calculate the specific heat in a consistent way [22].

Above all, we go over traditional translational symmetry and Bloch's theorem [23].

The hamiltonian of a system with the translational symmetry is expressed as

$$H = -\frac{\hbar^2}{2\mu}\nabla^2 + V(\mathbf{r}); \quad V(\mathbf{r} + \mathbf{R}_j) = V(\mathbf{r}), \tag{18}$$

where $\mathbf{R}_j = n_{j1}\mathbf{a}_1 + n_{j2}\mathbf{a}_2 + n_{j3}\mathbf{a}_3$ and n_{j1}, n_{j2}, n_{j3} are integers.

Define translational operators $\mathcal{J}(\mathbf{R}_j)$, which act on a function $f(\mathbf{r})$ as:

$$\mathcal{J}(\mathbf{R}_j) f(\mathbf{r}) = f(\mathbf{r} + \mathbf{R}_j). \tag{19}$$

It follows that

$$\mathcal{J}(\mathbf{R}_j)\mathcal{J}(\mathbf{R}_l) = \mathcal{J}(\mathbf{R}_l + \mathbf{R}_j) = \mathcal{J}(\mathbf{R}_j + \mathbf{R}_l) = \mathcal{J}(\mathbf{R}_l)\mathcal{J}(\mathbf{R}_j), \tag{20}$$

and

$$\begin{aligned}\mathcal{J}(\mathbf{R}_j)Hf(\mathbf{r}) &= -\frac{\hbar^2}{2\mu}\mathcal{J}(\mathbf{R}_j)\nabla^2 f(\mathbf{r}) + \mathcal{J}(\mathbf{R}_j)V(\mathbf{r})f(\mathbf{r}) \\ &= -\frac{\hbar^2}{2\mu}\nabla^2\mathcal{J}(\mathbf{R}_j)f(\mathbf{r}) + V(\mathbf{r}+\mathbf{R}_j)f(\mathbf{r}+\mathbf{R}_j) \\ &= [-\frac{\hbar^2}{2\mu}\nabla^2 + V(\mathbf{r})]f(\mathbf{r}+\mathbf{R}_j) = H\mathcal{J}(\mathbf{R}_j)f(\mathbf{r}).\end{aligned} \tag{21}$$

Therefore $\{\mathcal{J}(\mathbf{R}_j), H\}$ is the set of conserved quantities. In this case, an eigenfunction of the Hamiltonian must be an eigenfunction of the translational operators, i.e., $\mathcal{J}(\mathbf{R}_j)\psi(\mathbf{r}) = \psi(\mathbf{r}+\mathbf{R}_j) = \lambda(\mathbf{R}_j)\psi(\mathbf{r})$ if $H\psi(\mathbf{r}) = E\psi(\mathbf{r})$. Furthermore, the electron density must be periodic, i.e., $|\psi(\mathbf{r}+\mathbf{R}_j)|^2 = |\psi(\mathbf{r})|^2$. It follows that

$$|\lambda(\mathbf{R}_j)|^2 = 1. \tag{22}$$

But from Eq.(20), we know

$$\lambda(\mathbf{R}_j)\lambda(\mathbf{R}_l) = \lambda(\mathbf{R}_j + \mathbf{R}_l). \tag{23}$$

The solution of Eq.(23) under the constraint Eq.(22) is $\lambda(\mathbf{R}_j) = e^{i\boldsymbol{\kappa}\cdot\mathbf{R}_j}$. Thus we have Bloch's theorem:

$$\psi(\mathbf{r}+\mathbf{R}_j) = e^{i\boldsymbol{\kappa}\cdot\mathbf{R}_j}\psi(\mathbf{r}). \tag{24}$$

Next, we will turn to the spiral symmetry and generalize the Bloch's theorem. The hamiltonian with the spiral symmetry in cylindrical coordinates is expressed:

$$H = -\frac{\hbar^2}{2\mu}(\frac{\partial^2}{\partial r^2} + \frac{\partial}{r\partial r} + \frac{\partial^2}{r^2\partial\theta^2} + \frac{\partial^2}{\partial z^2}) + V(r,\theta,z), \tag{25}$$

$$V(r,\theta,z) = V(r,\theta + j_1\vartheta, z + j_1\tau + j_2 T), \tag{26}$$

where $\vartheta = 2\pi/N, N\tau = MT$, $N, M \in \mathbb{N}$, $j_1, j_2 \in \mathbb{Z}$. Define vectors $\mathbf{r} = (\theta, z)$, $\mathbf{R}_j = (j_1\vartheta, j_1\tau + j_2 T)$ in the space $[0, 2\pi) \times \mathbb{R}$, and operators $\mathcal{J}(\mathbf{R}_j)$ which act on a function $f(r;\mathbf{r})$ as $\mathcal{J}(\mathbf{R}_j)f(r;\mathbf{r}) = f(r;\mathbf{r}+\mathbf{R}_j)$. It follows that $\mathcal{J}(\mathbf{R}_j)\mathcal{J}(\mathbf{R}_l) = \mathcal{J}(\mathbf{R}_l + \mathbf{R}_j) = \mathcal{J}(\mathbf{R}_j + \mathbf{R}_l) = \mathcal{J}(\mathbf{R}_l)\mathcal{J}(\mathbf{R}_j)$ and $\mathcal{J}(\mathbf{R}_j)V(r;\mathbf{r}) = V(r;\mathbf{r})\mathcal{J}(\mathbf{R}_j)$. Otherwise,

$$\mathcal{J}(\mathbf{R}_j)(\frac{\partial^2}{r^2\partial\theta^2} + \frac{\partial^2}{\partial z^2})f(r;\mathbf{r}) = (\frac{\partial^2}{r^2\partial\theta^2} + \frac{\partial^2}{\partial z^2})\mathcal{J}(\mathbf{R}_j)f(r;\mathbf{r}). \tag{27}$$

Thus

$$\mathcal{J}(\mathbf{R}_j)H = H\mathcal{J}(\mathbf{R}_j). \tag{28}$$

We can obtain generalized Bloch's theorem analogizing the method to obtain the traditional Bloch's theorem:

$$\psi(r;\mathbf{r}+\mathbf{R}_j) = e^{i\boldsymbol{\kappa}\cdot\mathbf{R}_j}\psi(r;\mathbf{r}), \tag{29}$$

where $\boldsymbol{\kappa} = (l, \kappa)$, $l = 0, 1, \cdots, N-1$, $\quad 0 \leq \kappa < 2\pi/T$.

If we set $\boldsymbol{\alpha}_1 = (\vartheta, \tau)$, $\boldsymbol{\alpha}_2 = (0, T)$, $\boldsymbol{\beta}_1 = (N, 0)$, $\boldsymbol{\beta}_2 = (-\tau N/T, 2\pi/T)$, $\mathbf{G_j} = j_1\boldsymbol{\beta}_1 + j_2\boldsymbol{\beta}_2 = (j_1 N - j_2 N\tau/T, 2\pi j_2/T)$, then we can expand the wave function as the superposition of planar waves:

$$\psi(r; \mathbf{r}) = \sum_{\mathbf{j}} C_{\mathbf{j}} \varphi(r) e^{i(\boldsymbol{\kappa} + \mathbf{G_j})\cdot \mathbf{r}}. \tag{30}$$

In cylindrical coordinates, Eqs.(29) and (30) are expressed

$$\psi(r, \theta + \frac{2\pi j_1}{N}, z + j_1\tau + j_2 T) = e^{i[\frac{2\pi l j_1}{N} + \kappa(j_1\tau + j_2 T)]}\psi(r, \theta, z), \tag{31}$$

$$\psi_{l\kappa}(r, \theta, z) = \sum_{j_1 j_2} C_{j_1 j_2} \varphi_{l\kappa}(r) e^{i[(l + j_1 N - j_2 N\tau/T)\theta + (\kappa + 2\pi j_2/T)z]}. \tag{32}$$

If Expanding $\varphi_{l\kappa}(r)$ with normalized orthogonal basis $\{\chi_{nl\kappa}(r), n \in \mathbb{N}\}$ we obtain the secular equation from Eq.(32) and Shrödinger equation

$$det[(\mathcal{H}_{m_1 m_2 j_1 j_2 n n'} - E_{nl\kappa}\delta_{j_1 m_1}\delta_{j_2 m_2}\delta_{nn'})] = 0, \tag{33}$$

where $\mathcal{H}_{j_1 j_2 m_1 m_2 n n'} = \mathcal{T}_{j_1 j_2 n n'}\delta_{j_1 m_1}\delta_{j_2 m_2} + \mathcal{U}_{j_1 j_2 m_1 m_2 n n'}$, $\mathcal{T}_{j_1 j_2 n n'} = -\frac{\hbar^2}{2\mu}\int_0^\rho \chi_{nl\kappa}(r)[\frac{d^2}{dr^2} + \frac{d}{rdr} - \frac{(l + j_1 N - \frac{j_2 N\tau}{T})^2}{r^2} - (\kappa + \frac{2\pi j_2}{T})^2]\chi_{n'l\kappa}(r) r dr$, and
$\mathcal{U}_{j_1 j_2 m_1 m_2 n n'} = \frac{N}{2\pi T}\int_0^{2\pi} d\theta \int_0^T dz \int_0^\rho r dr \chi_{nl\kappa}(r) U(r, \theta, z) \chi_{n'l\kappa}(r) e^{i[(j_1 - m_1) - \frac{(j_2 - m_2)\tau}{T}]N\theta + \frac{i2\pi(j_2 - m_2)z}{T}}$.

References

[1] Iijima S 1991 *Nature* **354** 56

[2] Hamada N, Sawada S I and Oshiyama A 1992 *Phys. Rev. Lett.* **68** 1579; Saito R, Fujita M, Dresselhaus G and Dresselhaus M S 1992 *Appl. Phys. Lett.* **60** 2204; Mintmire J W, Dunlap B I and White C T 1992 *Phys. Rev. Lett.* **68** 631

[3] Yakobson B I and Avouris P 2001 *Mechanical Properties of Carbon Nanotubes, in Carbon Nanotubes* edited by Dresselhaus M S and Avouris P (Berlin: Springer-Verlag) pp 287

[4] Ou-Yang Z C, Su Z B and Wang C L 1997 *Phys. Rev. Lett.* **78** 4055; Tu Z C and Ou-Yang Z C 2002 *Phys. Rev.* B **65** 233407

[5] Dillon A C, Jones K M, Bekkedahl T A, Kiang C H, Bethune D S and Heben M J 1997 *Nature* **386** 377 ; Liu C, Fan Y Y, Liu M, Cong H T, Cheng H M and Dresselhaus M S 1999 *Science* **286** 1127

[6] Teizer W, Hallock R B, Dujardin E and Ebbesen T W 1999 *Phys. Rev. Lett.* **82** 5305; 2000 *Phys. Rev. Lett.* **84** 1844; Kuznetsova A, Yates J T, Liu J and Smalley R E 2000 *J. Chem. Phys.* **112** 9590; Talapatra S, Zambano A, Weber S E and Migone A D 2000 *Phys. Rev. Lett.* **85** 138

[7] Calbi M, Cole M W, Gatica S, Bojan M J and Stan G 2001 *Rev. Mod. Phys.* **73** 857; Calbi M and Cole M W 2002 *Phys. Rev.* B **66** 115413; Stan G, Gatica S, Boninsegni M, Curtarola S and Cole M W 1999 *Am. J. Phys.* **67** 1170

[8] Carraro C 2000 *Phys. Rev.* B **61** R16351; Zambano A J, Talapatra S and Migone A D 2001 *Phys. Rev.* B **64** 75415; Gordillo M C, Boronat J and Casulleras J 2000 *Phys. Rev. Lett.* **85** 2348

[9] Tu Z C and Ou-Yang Z C 2002 *Preprint* cond-mat/0211658

[10] Šiber A and Buljan H 2002 *Phys. Rev.* B **66** 75415; Šiber A 2002 *Phys. Rev.* B **66** 205406

[11] Saito R, Dresselhaus M S and Dresselhaus G 1998 *Physical Properties of Carbon Nanotubes* (London: Imperial College Press)

[12] Hirschfelder J O, Curtiss C F and Bird R B 1954 *Molecular Theory of Gases and Liquids* (New York: John Wiley & Sons Inc.)

[13] An R Private communication; Peng H H and Xu X S 1998 *The Fundamentals of Theoretical Physics* (Beijing: Peking University Press)
[14] Landau L D and Lifshitz E M 1986 *Statistical Physics* (Oxford: Pergamon); Reichl L E 1998 *A Modern Course in Statistical Physics* (New York: John Wiley & Sons, Inc.)
[15] Landau L D and Lifshitz E M 1986 *Quantum Mechanics* (Oxford: Pergamon)
[16] Wang Z X and Guo D R 2000 *Introduction to Special Function* (Beijing: Peking University Press)
[17] Kittel C 1996 *Introduction to Solid State Physics* (New York: John Wiley & Sons, Inc.)
[18] In fact, here we just consider the energies in the first Brillouin zone. If considering $E_{\boldsymbol{\kappa}} = E_{-\boldsymbol{\kappa}}$ and $E_{\boldsymbol{\kappa}} = E_{\boldsymbol{\kappa}+\mathbf{G}_j}$, we need to multiple a constant before the partition function $\mathcal{Z}$ in the expression of the free energy.
[19] Calbi M M, Gatica S M, Bojan M J and Cole M W 2002 *Preprint* cond-mat/0209220
[20] Gay J G and Berne B J 1981 *J. Chem. Phys.* **74** 3316
[21] Hansen J P and McDonald I R 1976 *Theory of Simple Liquids* (New York: Academic Press)
[22] Tu Z C 2002 *Preprint* cond-mat/0212003
[23] Callaway J 1991 *Quantum Theory of the Solid State* (London: Academic Press Inc.)

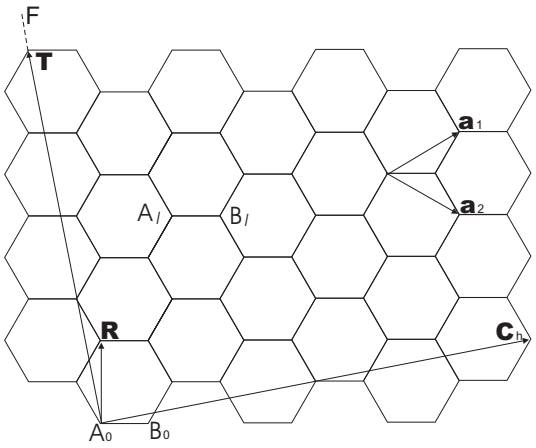


Figure 1. The unrolled honeycomb lattice of a SWNT. By rolling up the sheet along the chiral vector $\mathbf{C}_h$, that is, such that the point A_0 coincides with the point corresponding to vector $\mathbf{C}_h$, a nanotube is formed. The vectors $\mathbf{a}_1$ and $\mathbf{a}_2$ are the real space unit vectors of the hexagonal lattice. The translational vector $\mathbf{T}$ is perpendicular to $\mathbf{C}_h$ and runs in the direction of the tube axis. The vector $\mathbf{R}$ is the symmetry vector. A_0, B_0 and $A_l, B_l (l = 1, 2, \cdots, N)$ are used to denote the sites of carbon atoms.

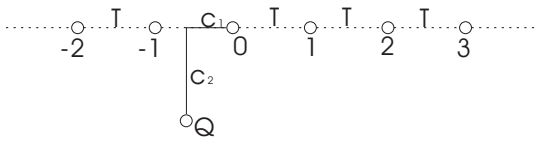


Figure 2. An infinite atom chain and an atom Q out of the chain. Many atoms distribute regularly in a line form the infinite atom chain. The interval between neighbor atoms in the chain is T, and the site of atom Q relative to atom 0 can be represented by numbers c_1 and c_2.

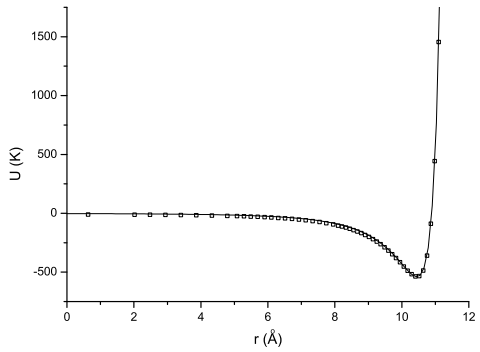


Figure 3. The potentials inside the $(20, 20)$ nanotube calculated from Eq.(7) (squires) and the fit curve (solid curve).

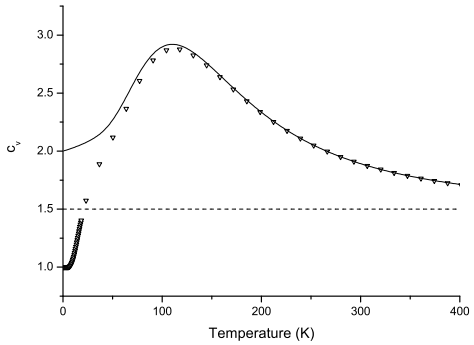


Figure 4. The specific heats per atom c_v of Ne inside $(20, 20)$ nanotube at different temperatures without considering the θ, z effect. The triangles is the results of OS and the solid line is that of CSM.

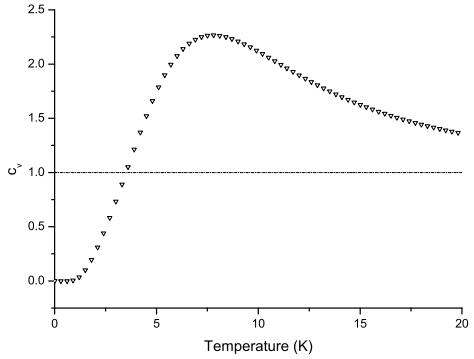


Figure 5. The specific heats (triangles) per atom c_v of Ne inside $(20, 20)$ nanotubes at low temperatures.

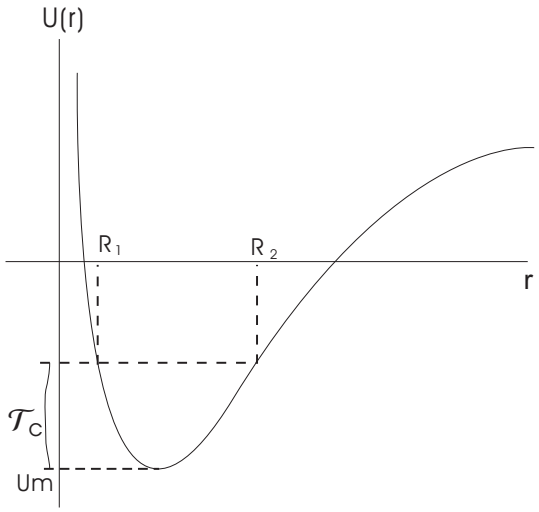


Figure 6. A potential and its characteristic temperature. U_m is the minimum of the potential and $\mathcal{T}_c$ is the characteristic temperature. The parameters R_1 and R_2 satisfy $U(R_1) = U(R_2) = U_m + \mathcal{T}_c$.

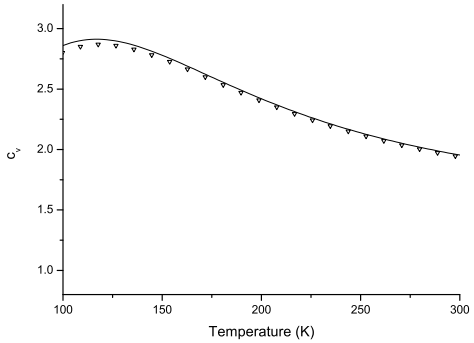


Figure 7. The specific heats per atom c_v of Ne inside $(20, 20)$ nanotube at high temperatures. The triangles is the results of OS without considering the θ, z effect and the solid line is that of CSM with the θ, z effect.